Bottom-up simulation calibration of zone and system level models using building automation system (BAS) trend data

Nicholas Zibin[1], Radu Zmeureanu[1], and James Love[2]
[1] Center for Zero Energy Building Studies, Department of Building, Civil, and Environmental Engineering, Concordia University Montreal, Quebec
[2] Faculty of Environmental Design, University of Calgary, Calgary, Alberta

Abstract

The bottom-up calibration approach sequentially calibrates the zone, system, plant, and whole-building level models. The approach was applied to an eQUEST model on a zone and system level of a university research center using building automation system (BAS) trend data. This study focused on the shoulder season when the heating and cooling coils in air handling units (AHUs) were inactive. The zone level models' coefficient of variation of root-mean-squared error (CV-RMSE) for indoor air temperatures and supply air flow rates ranged from 3-6 % and 3-34 %, respectively, with the exception of two zones that did not fit the BAS trend data well. Calibrating the zone level models first and using system level inputs generated from BAS trend data resulted in calibrated system level AHU temperatures, supply air flow rates, and heat recovery heat flow rates with a CV(RMSE) of 7-19%, 11%, and 25%, respectively.

1 Background

Calibrated building energy models can be used to identify energy efficiency measures, create benchmarks for operation, perform fault detection and diagnostics (O'Neill et al. 2013), and estimate future performance under new operating conditions. A calibrated building energy model generates estimates that match the measured energy use with acceptable accuracy. Reddy (2006) noted that a key issue in calibration is uncertainty due to offsetting errors caused by the resolution of calibration in terms of time and/or end use (i.e., if limited to monthly utility data). Raftery et al. (2011) used short-term (sub-hourly) data and although the scope was limited to electrical end uses, subsystem electrical data were collected via a dedicated monitoring system. They also advocated more explicit documentation of the tuning process.

Calibration methods have been applied to both simplified (Liu, M & Liu, G 2011; Heo et al. 2012) and detailed models (Monfet et al. 2009; Raftery et al. 2011; Kandil and Love 2013; Mihai & Zmeureanu 2013; Gestwick and Love 2013). Heo et al. (2012) showed that simplified models could be as accurate as detailed models at the whole building level. However, Raftery et al. (2011) argued that simplified models could not represent energy efficiency measures at the zone, system, and plant levels. Raftery et al (2011) and Kandil & Love (2013) showed that sub-monthly sub-utility measurements revealed calibration errors would have occurred if only monthly utility data was used. Gestwick & Love (2013) found substantial discrepancies between measured and simulated heating plant performance which could have led to erroneous tuning (e.g., heat recovery effectiveness) if plant level measurements were unavailable.

Use of BAS trend data for calibration was reported by Carling et al. (2003) as early as 2003, with more attention in recent years (Monfet et al. 2009; Gestwick & Love 2013; Kandil

& Love 2013; Mihai & Zmeureanu 2013; O'Neill et al. 2013). A barrier is that the time and effort required is much larger than that required to analyze whole-building utility data. As Torcellini et al (2006, p. 102) noted "with current EMS [energy management systems] and building automation systems there appears to be a low probability of obtaining contiguous error-free, measured data sets over a very long period." They recommended dedicated systems for sub-utility monitoring. However, this presents challenges in terms of additional cost and complexity.

Most studies of calibration methods have used a top-down approach with deductive reasoning, assuming that if the whole-building level model was calibrated, then the plant, system and zone level models were likely to be calibrated. Some more recent studies have augmented this with subsystem verification (Monfet et al. 2009; Raftery et al. 2011, Gestwick & Love 2013; Kandil & Love 2013). Mihai & Zmeureanu (2013) and Zibin et al. (2013) proposed a bottom-up calibration procedure that involved sequentially calibrating zone, system, plant, and whole building level models (Figure 1).

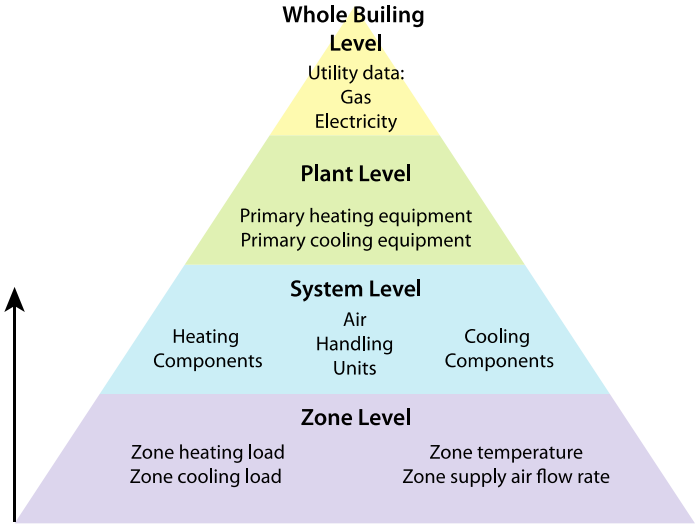

Figure 1. Bottom-up simulation calibration approach (Zibin et al. 2013)

The number of measurement points to be considered for analysis in bottom-up simulation calibration is very large. Building automation system (BAS) trend data, which is extensive in many commercial and institutional buildings, could provide some of the required measurement points. BAS trend data typically includes air and thermofluid temperatures, air humidity, and air flow rates; rarely are thermofluid flow rates and sub-hourly electric demand available. In addition, there are some phenomena that may be highly influential in energy use, such as occupant numbers, infiltration, and foundation heat loss, but are particularly difficult to measure on an ongoing basis.

To reduce time and effort required for BAS trend data analysis, a proof-of-concept prototype, called the Automatic Assisted Calibration System (AACS) was developed (Zibin et al. 2013). This automatically generated some values from BAS trend data for use as inputs in the building simulation model. Unlike programs that automatically create a calibrated model by tuning inputs based on an optimization approach, such as SIMEB (Millette et al. 2013), it is limited to providing calibration assistance.

Throughout the three decades of research into simulation calibration, a basic issue has remained: the number of model inputs required to characterize building performance exceeds the number of measured points (Sun & Reddy 2006). This issue was addressed by using a large BAS trend database to increase the number of known inputs and by attempting model

calibration for a shoulder season when the heating and cooling coils in the air handling units (AHUs) were inactive in order to further simplify the model.

2 Method

The bottom-up calibration procedure proposed here (Figure 1) uses inductive reasoning based on evidence from BAS trend data. If the zone, system, plant, and whole-building level models are calibrated, then the model is likely to be a good representation of the building. The hypothesis is that bottom-up calibration can create more accurate and reliable models than those using top-down approaches. Bottom-up calibration includes four main steps, depending on available measurements:

1. Zone level model calibration is addressed first, including zone air temperatures, air flow rates, and cooling/heating loads.
2. System level models, including the AHU components such as supply, mixed, return air temperatures (T_s, T_m, T_r), supply, return, and exhaust air flow rates, fan power and heating/cooling components (e.g., heating/cooling coil heat flow rates, thermofluid temperatures and flow rates).
3. Plant level model including heating and cooling primary equipment.
4. The whole-building level model using utility data.

This paper breaks away from traditional calibration of the whole-building level and instead focuses on calibration of the zone and system level models (i.e., steps 1 and 2 above) of a case study building. The available BAS trend data in this case study allowed for calibration of zone level indoor air temperatures and supply air flow rates and system level calibration of T_s, T_m, T_r, supply air flow rates, and heat recovery heat flow rates in the AHUs.

The most common measure of the representativeness of a simulation model is the ASHRAE (2002) Guideline 14 goodness of fit criteria, mean bias error (MBE) (Equation 1) and the coefficient of variation of root-mean-squared error (CV-RMSE) (Equation 2 and 3). MBE indicates the degree of spread between measured and estimated values, for the period of interest. The CV(RMSE) quantifies the match while accounting for offsetting positive and negative errors. Guideline 14's maximum MBE and CV(RMSE) are 10% and 30%, respectively, for hourly data.

$$MBE = \frac{\sum_{i=1}^{n}(\hat{x}_i - x_i)}{\sum_{i=1}^{n} x_i} \quad (1)$$

$$RMSE = \sqrt{\frac{\sum_{i=1}^{n}(\hat{x}_i - x_i)^2}{n-1}} \quad (2)$$

$$CV(RMSE) = \frac{RMSE}{\bar{x}} \quad (3)$$

where: x, $\hat{x}$, and $\bar{x}$ are the sampled data, predicted data, and the mean of the sampled data, respectively; and
n is the number of samples

3 Building Description

The case study building was the Research Centre for Structural and Functional Genomics ("Genome Building") located on Concordia University Loyola Campus in Montreal, Canada (Figure 2). The building was completed in 2011 and was certified LEED Gold in 2013. It has a floor area of 5200 m^2, consisting of 5 levels, including a basement and a mechanical penthouse. The building has an orientation of approximately 60° west of north and a window-to-wall ratio of 33%. The building houses laboratories, offices, and conference rooms.

The Genome Building has a variable-air-volume (VAV) system. Two identical air-handling units (AHUs), connected in parallel, have a total supply air flow capacity of 42,500 L/s. The air within the AHUs is conditioned using run-around sensible heat recovery coils, heating coils, cooling coils, and steam humidification. Hot and chilled water are supplied from a campus central plant. Room supply air flow rates are controlled by VAV terminal units depending on the room temperature set point and occupancy. A detailed description may be found in Zibin et al. (2013).

Figure 2. The Genome Building located in Montreal, Canada

4 Initial Building Energy Model

The energy model was created in eQUEST (LBNL & JJH 1998) using information found via construction documents, visits and interviews with the operating team, and BAS trend data. eQUEST was chosen because it is one of the most widely used building simulation tools in North America, it is based on DOE-2 which has been extensively documented and validated.

Calibration was performed for April 8th to 21st, 2013. All inputs generated in the AACS using BAS trend data were calculated for this time period, unless otherwise stated. Weather data was obtained from Hydro Quebec's website (SIMEB 2013) using data collected at the Montreal-Pierre Elliot Trudeau International Airport, located approximately 9 km west from the Genome Building. The difference between the air temperature trend data recorded nearby, and the weather file had an MBE of -16%, a RMSE of 1.8 °C, and a CV-RMSE of 0.25.

Definition of building geometry and thermal zones

A total of 20 thermal zones (including 3 plenum zones) were defined based on space function, proximity to the exterior, and orientation. The basement floor was not modelled because it housed a large data center with dedicated chillers and cooling towers that would greatly increase model complexity. The mechanical penthouse and emergency staircase located on the SW face of the building were excluded to further simplify the model. The excluded features were replaced with adiabatic surfaces. Shading from nearby buildings to the north and northwest and the vertical fenestration fins were included.

Definition of envelope assemblies

The walls (brick and aluminum panel) were defined based on the specifications and thermal resistance of envelope assemblies stated in construction documents, and material characteristics from (ASHRAE 2009). Thermal bridging in the aluminum panel wall was accounted for using the method in Appendix C of NRC (1997). The modelled U-values of the brick and aluminum panel walls were 0.27 and 0.36 W/m^{2}K, respectively.

The visible section of the curtain wall was modelled as green-tinted double-glazed with a 12.7 mm air gap. The solar and optical window properties for the center-of-glass were obtained from the eQUEST library for glazing type 2210. The overall visible curtain wall U-value (3.5 W/m^{2}K) was calculated by accounting for the edge-of-glass and frames coefficients (ASHRAE 2009). The opaque section of the curtain wall was modelled with a U-value of 0.74 W/m^{2}K.

Definition of internal loads

Lighting and equipment loads are rarely sub-metered and occupant loads are difficult to measure unless time clock or security card records are available (Haves et al. 2001). Lighting and plug loads were not sub-metered and occupancy was not tracked. The lighting and equipment power could have been surveyed, but lack of sub-metering demand patterns still results with uncertain hourly magnitudes.

Lighting, equipment, and occupancy (referred to herein as internal loads) peak values and schedules were estimated using values found in the literature for use as a starting point in the initial model. These values could be tuned during calibration if necessary. Equipment power densities for all space types were estimated using ASHRAE (2009). Lighting power densities for all space types were estimated using ASHRAE 90.1 (2010). The maximum occupancy density by space type was estimated based on values in ASHRAE 62 (2001), while corresponding sensible heat gains were obtained from ASHRAE (2009).

To the authors' knowledge no lighting and equipment schedules have been published for university research buildings similar to the Genome Building. These were therefore estimated using the schedules created by Claridge et al. (2004) for office buildings. The occupancy schedules developed by Davis and Nutter (2010) for a university research center were used. To simplify the calibration of internal loads because of their large uncertainty, the effect of several internal loads was replaced with one single internal load. The lighting, equipment, and occupancy loads were summed to create a single peak value for each zone and schedules were aggregated into a weekend and weekday schedule used for all zones in the model.

Infiltration was assumed to be zero because the fans continuously create a positive pressure except for 10% of the exterior wall area in negatively pressured laboratories.

Definition of thermal zone inputs

Table 1 shows the zone level inputs generated for the second floor in the AACS based on BAS trend data. The maximum reheat temperature provided by the VAV terminals was estimated as 11.2 °C from the maximum difference between zone T_s (measured only in two rooms) and AHU T_s.

Table 1. Initial zone model inputs generated from BAS trend data for the second floor

Zone	Average zone temperature (°C)				Supply Air Flow (L/s)	
	Weekday		Weekend			
	Day	Night	Day	Night	Design	Min Flow ratio
Z2-SW	23.0	21.8	22.4	21.5	1340	0.28
Z2-E	22.2	22.2	22.2	22.2	2490	0.38
Z2-INT	23.0	22.9	22.9	22.8	500	0.44
Z2-NE	22.6	21.4	21.3	21.0	1870	0.48
Z2-S	22.4	22.4	22.4	22.3	490	0.81
Z2-W	23.0	22.2	21.9	21.7	310	0.00

Definition of system level components

The system was modelled as a variable air volume (VAV) system with zone hot water reheat. Table 2 shows the system level inputs that were generated in the AACS using BAS trend data. The maximum design air flow rate was calculated as the maximum of the sum of zone supply air flow rates because only 3 out of 4 floors were modelled. Return air relative humidity (RH) was measured in the return air ducts of the AHUs. The economizer control was specified as dual enthalpy because the economizer operates when the enthalpy of the outside air is less than the return air enthalpy. A sensible energy recovery ventilator with outdoor air bypass was used to model the run-around heat recovery coils. Heat recovery was activated when the outside air temperature was less than 8 °C. Because no heating or cooling coils were activated during this study the T_s was controlled as a function of the heat recovery outlet air temperature and position of the mixing air dampers.

Table 2. Initial system level model inputs generated from BAS trend data

Description	Value	Unit
Maximum design air flow rate	16100	L/s
Minimum supply air flow ratio	0.52	-
ΔT_{fan}	1.8	°C
Maximum return air relative humidity	26.7	%
Minimum return air relative humidity	25.4	%
Heat recovery outlet air temperature	9.4	°C
Minimum OA ratio	58	%

Initial zone level model results

Hourly values extracted from eQUEST were compared to hourly averaged BAS trend data. The initial zone level model results for the second floor are shown in Table 3. The simulated zone air temperatures were generally lower than measured values whereas the zone supply air flow rates were higher. For example, in the case of a north east facing thermal zone (Z2-NE) consisting of offices and a small laboratory, the indoor air temperature followed the pattern of variation showed by measurements (Figure 3) but at a consistently lower value. The variation of simulated supply air flow rate (M_s) differed from the pattern shown in the trend data (Figure 4).

Table 3. Statistical comparison of initial zone level models to BAS trend data

Zone	Temperature			Supply air flow	
	MBE	RMSE (°C)	CV(RMSE)	MBE	CV(RMSE)
Z2-SW	-0.10	2.5	0.11	0.26	0.76
Z2-E	-0.06	1.5	0.07	-0.03	0.43
Z2-INT	-0.07	1.8	0.08	0.14	0.42
Z2-NE	-0.09	2.1	0.10	0.23	0.46
Z2-S	-0.10	2.4	0.11	-0.04	0.12
Z2-W	-0.10	2.3	0.10	1.3	2.3

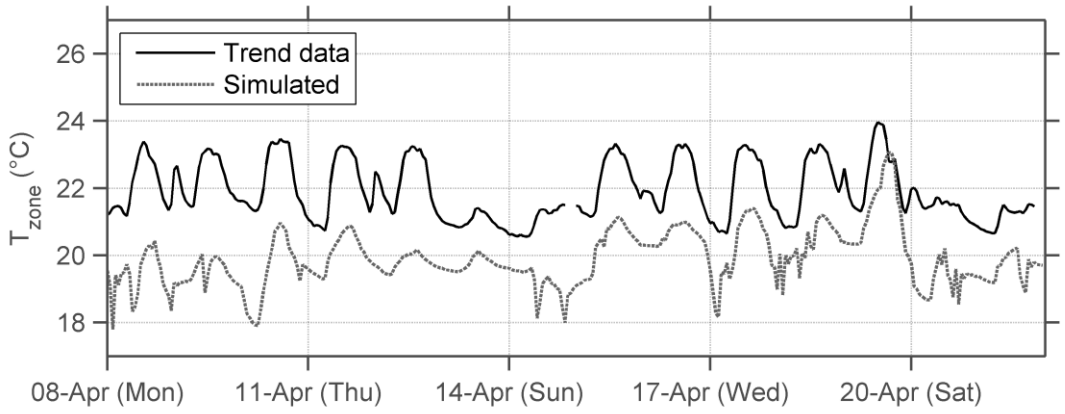

Figure 3. Zone Z2-NE initial model indoor air temperature

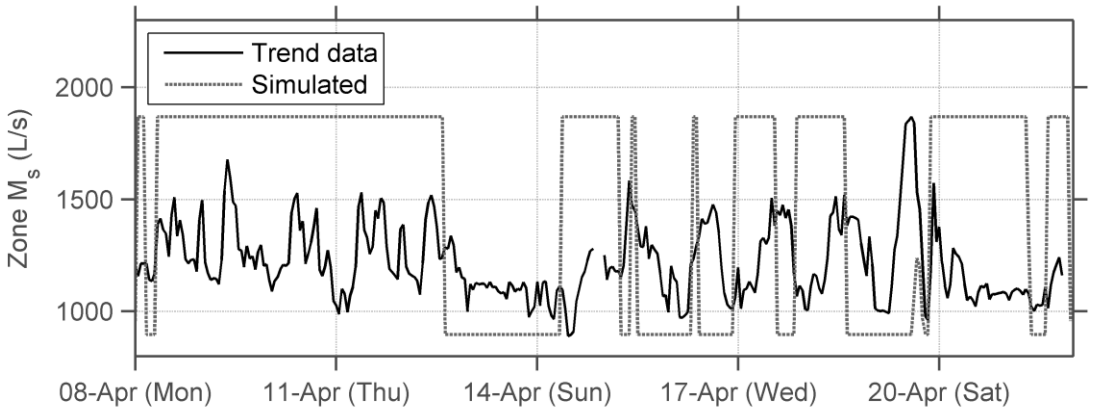

Figure 4. Zone Z2-NE initial model supply air flow rate

5 Calibrated Building Energy Model

Improved model: use of hourly inputs generated from BAS trend data

Existing building simulation software lacks the capacity to easily handle inputs of hourly BAS trend data (e.g., indoor air temperature and supply air flow rate) in a manner similar to hourly weather files. For this reason, the hourly average measured indoor air temperature extracted from the BAS trend data for each thermal zone were entered into the hourly thermostat set point schedules in eQUEST; one for the weekdays (WD) and a second for the weekends and holidays (WEH). An example of an hourly thermostat set point schedule for zone Z2-NE is shown in Figure 5.

An air flow rate schedule cannot be directly entered into eQUEST; however, hourly zone minimum flow ratio schedules can. Entering a minimum air flow ratio schedule forces the zone model's air flow rate to *at least* the air flow rate calculated from multiplying the maximum air flow rate by the specified minimum air flow ratio. This approach was used to emulate the input of hourly supply air flow rates in eQUEST for each thermal zone. Hourly average minimum supply air flow ratios for every zone were generated for weekdays and weekends/holidays from BAS trend data, and were entered into the model. An example of a minimum air flow ratio schedule (for zone Z2-NE) is shown in Figure 6. The improved zone level model results for the second floor are shown in Table 4.

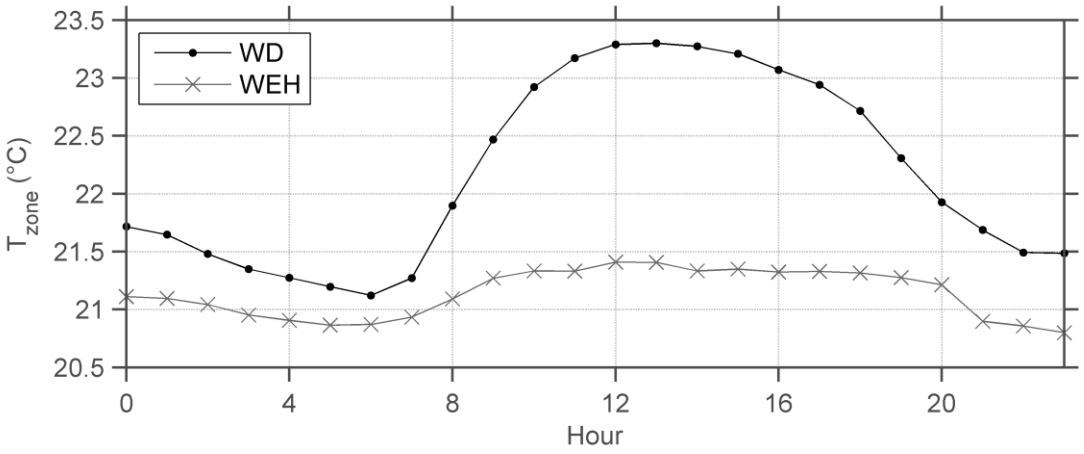

Figure 5. Hourly thermostat set point schedule for zone Z2-NE

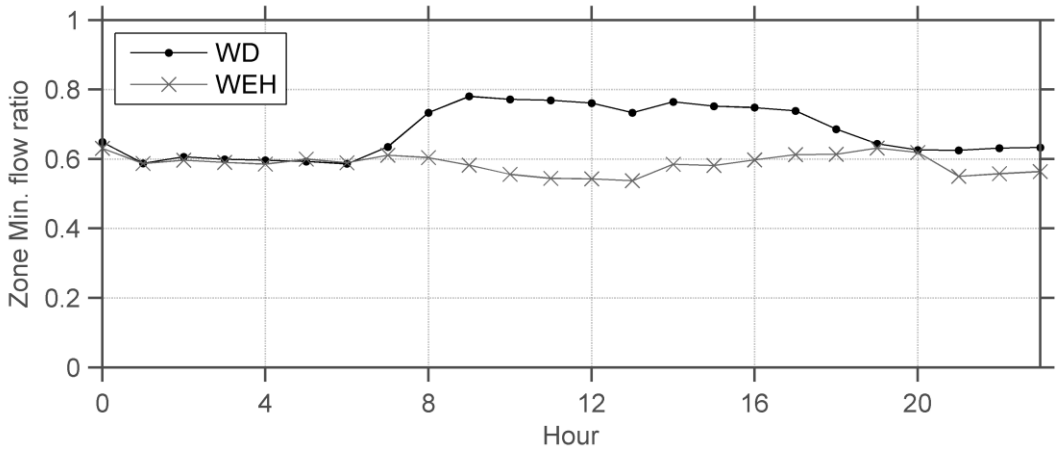

Figure 6. Hourly minimum air flow ratio schedule for zone Z2-NE

Although the improved zone level models' MBE and CV(RMSE) values in Table 4 have improved from the initial model results, all zones on the 2nd floor except zone Z2-S exceeded the acceptable values of 10% and 30%, respectively.

Table 4. Statistical comparison of improved zone level models to BAS trend data

Zone	Temperature			Supply air flow rate	
	MBE	RMSE (°C)	CV(RMSE)	MBE	CV(RMSE)
Z2-SW	-0.10	2.4	0.11	0.31	0.53
Z2-E	-0.06	1.5	0.07	0.10	0.31
Z2-INT	-0.07	1.8	0.08	0.18	0.33
Z2-NE	-0.09	2.1	0.09	0.19	0.34
Z2-S	-0.10	2.3	0.10	0.01	0.04
Z2-W	-0.09	2.2	0.10	1.05	1.68

Initial and improved system level model results

A statistical comparison of the system level model fit, based on the initial and improved models, of T_s, T_m, and T_r, supply air flow rates (M_s), and heat recovery flow rates (q_{hr}) is shown in Table 5. The T_s trend data was calculated as the average T_s in the parallel AHUs.

The system level supply air flow rate trend data was calculated from the sum of zone supply air flow rates because only 3 out of 4 floors were modelled. The results show that system level temperatures were underestimated and M_s and q_{hr} were overestimated.

Table 5. Statistical comparison of initial and improved system level models

	Initial			Improved		
	MBE	RMSE	CV(RMSE)	MBE	RMSE	CV(RMSE)
T_s (°C)	-0.08	2.7	0.20	-0.04	2.5	0.18
T_m (°C)	-0.11	2.3	0.20	-0.13	2.4	0.21
T_r (°C)	-0.10	2.3	0.10	-0.10	2.4	0.10
M_s (L/s)	0.18	5060	0.44	0.20	3680	0.32
q_{hr} (kW)	0.07	46	0.56	0.02	34	0.41

Zone level model calibration

A strategy for tuning some factors affecting loads (e.g., internal gains, envelope thermal properties, zone reheat, infiltration, etc.) was applied to the improved model based on the differences between simulated and trend zone air temperatures and supply air flow rates:

- Simulated zone air temperatures less than trend data suggests tuning factors to increase loads
- Simulated zone air temperatures greater than trend data suggests tuning factors to decrease loads
- Zone supply air flow rate trend data less than the simulations suggests the applied minimum flow ratio schedule was not representative for the given hour/day
- Simulated zone supply air flow rate greater than the trend data suggests tuning factors to increase or decrease loads whether the zone model is in a heating or cooling mode, respectively

The improved model results showed that simulated perimeter zone air temperatures were all less than the trend data. When the perimeter zone models experienced a net heating load, the zone air flow rate was greater than the trend data. This suggested that the model's loads should be increased. This was also supported by the overestimated M_s and q_{hr} in the improved system level models. Based on earlier assumptions for envelope thermal resistance and infiltration, this suggested increasing the internal loads and/or the zone air reheat temperature. Different combinations of these inputs could create calibrated models. Tuning the internal gains and zone reheat will mainly affect whole building electricity use and heating energy, respectively.

One zone air reheat temperature was accepted in eQUEST, which applied to every zone. The improved model results suggest the initially specified zone reheat was too small. This was a reasonable conclusion because the value generated in the AACS was calculated using only two rooms. The zone reheat was tuned until all perimeter zone supply air flow rates fit the trend data well, which occurred with a zone air reheat temperature of 15.3 °C. Once this was adjusted, zone model air temperature and supply air flow rates fit well with trend data as shown in Table 6. Zone Z2-NE's air temperatures and supply air flow rates are shown in Figure 7 and 8. Most interior zone simulation results generally fit the trend data well.

The model could also be calibrated by tuning the internal loads and the zone reheat temperature. The zone air reheat temperature was increased to 13.6 °C which was the

maximum measured during the heating season (Jan 7th – Mar 31st, 2013) and the internal gains were tuned which resulted in another calibrated model shown in Table 6. The new zone air reheat temperature may or may not be representative during the shoulder season but at least it was indicated from measurements that may represent the maximum possible zone air reheat temperature. Internal gains were tuned by adjusting peak values and creating custom schedules for some zones.

Table 6. Statistical comparison of calibrated zone level models

Zone	Calibrated: tuned zone reheat				Calibrated: tuned reheat and internal gains			
	Temperature		Supply air flow rate		Temperature		Supply air flow rate	
	RMSE	CV(RMSE)	MBE	CV(RMSE)	RMSE	CV(RMSE)	MBE	CV(RMSE)
Z1-S	1.2	0.05	0.68	1.2	1.0	0.05	0.63	1.2
Z1-NE	-	-	-	-	-	-	-	-
Z1-NW	0.61	0.03	0.00	0.03	0.65	0.03	0.01	0.03
Z1-CORR	0.68	0.03	0.00	0.05	0.74	0.03	0.00	0.05
Z1-CONF	0.68	0.03	0.06	0.32	0.76	0.03	0.03	0.31
Z2-SW	1.3	0.06	0.04	0.15	1.1	0.05	0.07	0.21
Z2-E	0.65	0.03	0.01	0.25	0.69	0.03	0.02	0.27
Z2-INT	0.74	0.03	0.01	0.17	0.62	0.03	0.03	0.21
Z2-NE	0.75	0.03	0.00	0.08	0.75	0.03	0.01	0.08
Z2-S	0.87	0.04	0.00	0.01	0.66	0.03	0.01	0.03
Z2-W	0.70	0.03	0.28	0.63	0.57	0.03	0.45	0.85
Z3-SW	0.99	0.05	0.00	0.12	0.94	0.04	0.01	0.14
Z3-E	0.77	0.03	0.00	0.12	0.70	0.03	0.01	0.13
Z3-INT	0.85	0.04	0.02	0.18	0.76	0.03	0.07	0.27
Z3-NE	0.80	0.04	0.00	0.10	0.82	0.04	0.01	0.10
Z3-S	0.98	0.04	0.15	0.34	0.70	0.03	0.08	0.28
Z3-W	0.76	0.04	0.05	0.29	0.93	0.04	0.03	0.27

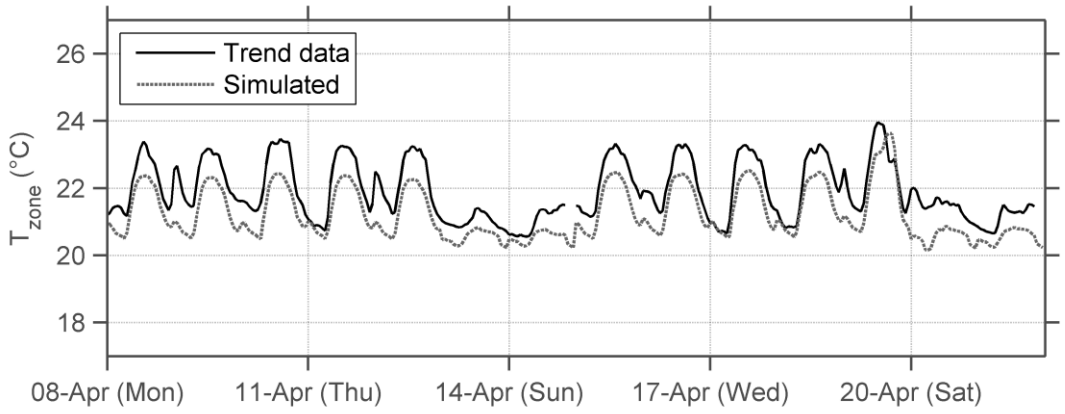

Figure 7. Calibrated zone Z2-NE indoor air temperature with tuned zone reheat

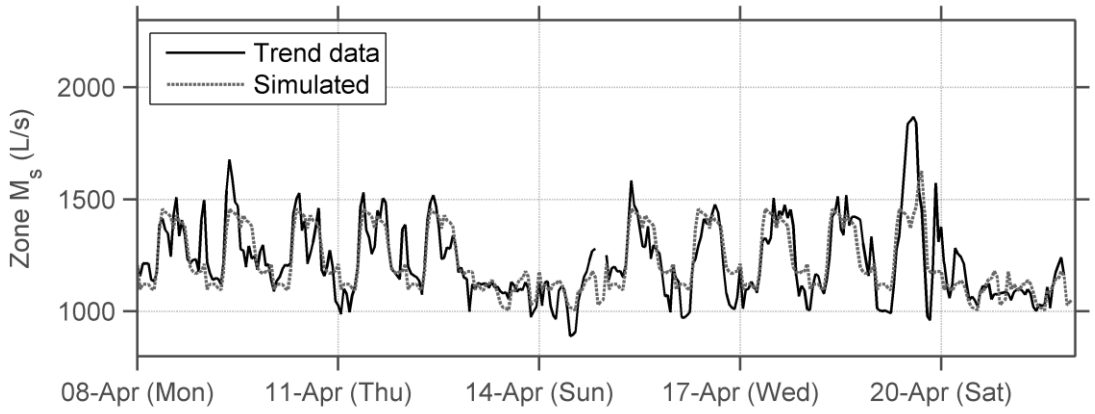

Figure 8. Calibrated zone Z2-NE supply air flow rate with tuned zone reheat

Tuning the internal gains in addition to the zone reheat resulted in one additional calibrated zone (Z3-S). Between the two tuning procedures, fit of some zone models improved, while others degraded.

There were a few zones that were not yet calibrated (Table 6). The supply air flow rate in zone Z1-S (offices) was not calibrated because applying the weekend hourly average thermostat set point schedule to this zone did not represent the lower indoor air temperature during the first weekend and the higher indoor air temperature during the second weekend. Similar issues occurred for zones that housed conference rooms or some laboratories, where meetings and experiments took place without a regular schedule (determined from supply air flow rates), causing errors in estimating the zone supply air flow rates.

System level calibration

A statistical comparison of model fit between the system level models, based on the two tuning procedures above, are shown in Table 7. Calibrating the zone level models first and using system level inputs generated from BAS trend data resulted in calibrated system level models for the period of analysis. The system level T_s, summation of zone supply air flow rates, and heat recovery heat flow rate are shown in Figures 9-11.

The differences between simulated zone supply air flow rates and the trend data during some nights and the weekend of April 12-13th are due to zone level supply air flow ratio schedules for some zones being poorly represented by the hourly average schedules for weekdays and weekends.

Table 7. Statistical comparison of calibrated system level models to BAS trend data

	Calibrated: tuned zone reheat			Calibrated: zone reheat and internal gains		
	MBE	RMSE	CV(RMSE)	MBE	RMSE	CV(RMSE)
T_s (°C)	-0.05	2.0	0.15	-0.06	2.2	0.16
T_m (°C)	-0.12	2.1	0.18	-0.13	2.1	0.19
T_r (°C)	-0.05	1.3	0.06	-0.07	1.8	0.07
M_s (L/s)	0.05	1080	0.10	0.04	1220	0.11
q_{hr} (kW)	0.09	21	0.26	0.05	21	0.25

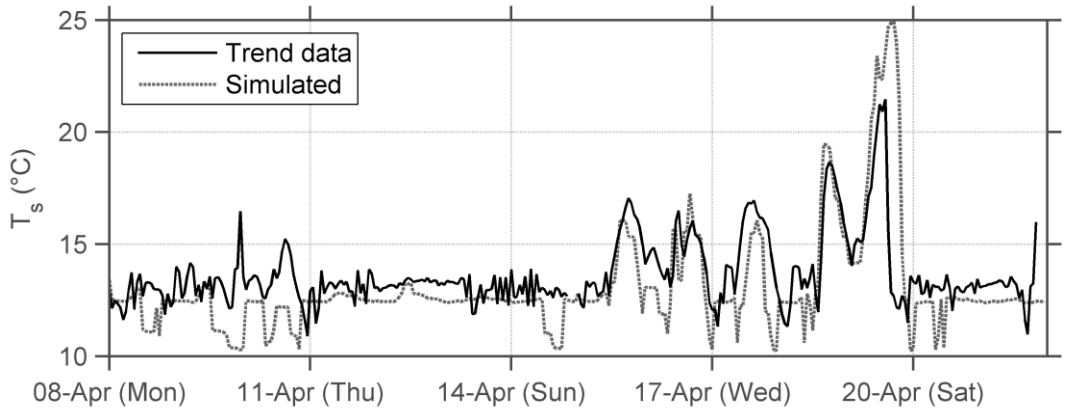

Figure 9. AHU supply air temperature calibrated with tuned zone reheat

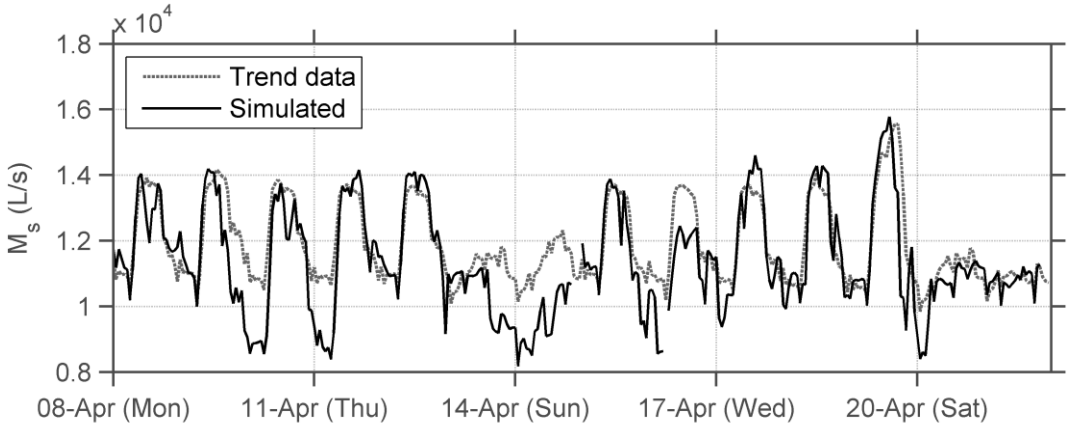

Figure 10. Sum of zone supply air flow rates calibrated with tuned zone reheat

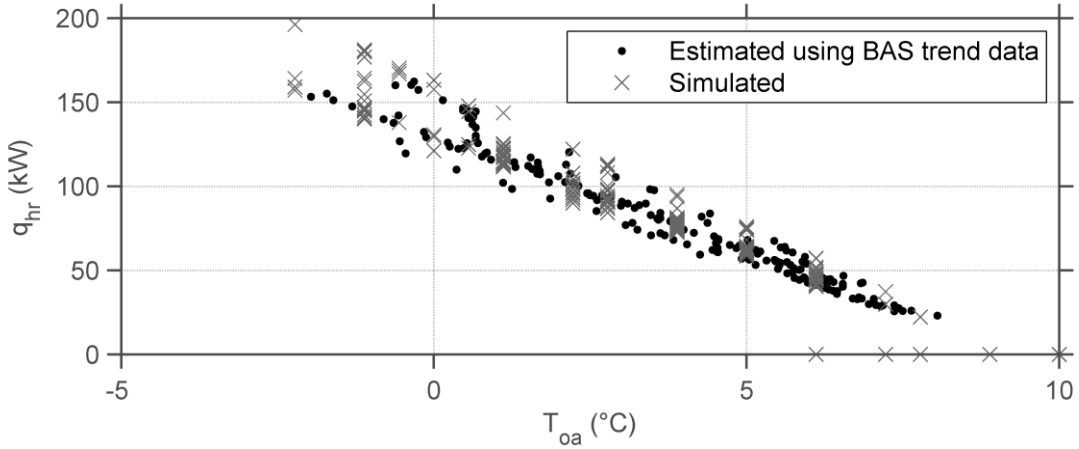

Figure 11. Heat recovery heat flow rate calibrated with tuned zone reheat

6 Conclusions

A bottom-up approach was used to calibrate an eQUEST model of a university research center using BAS trend data during a shoulder season. Shoulder season calibration, with inactive heating and cooling coils in the AHUs, made the trial bottom-up calibration more manageable. This exploratory study limited calibration to the zone and system level models within the whole building eQUEST model.

The first step in calibration began when the initial model was improved using hourly average temperature and minimum air flow ratio schedules generated from BAS trend data. Most zone level models were calibrated by tuning zone internal loads and/or zone reheat temperatures in the improved model. Simulation results were compared with BAS trend data using the MBE and CV(RMSE). The zone level models' CV(RMSE) for indoor air temperatures and supply air flow rates ranged from 3-6 % and 3-34 %, respectively, with the exception of two zones that did not fit the BAS trend data well. Calibrating the zone level models first and using system level inputs generated from BAS trend data resulted in calibrated system level models. System level AHU temperatures, supply air flow rates, and heat recovery heat flow rates had a CV(RMSE) of 7-19%, 11%, and 25%, respectively.

No data or publications are available to compare the accuracy and cost-effectiveness of whole-building calibration based on utility bills with the bottom-up approach. A main limitation of the bottom-up approach is the larger amount of time required to calibrate a substantial fraction of influential zones. However, the additional time spent on the calibration at sub-utility levels might be offset by revealing errors in BAS trend data, errors in key equipment performance models, and faults that may be difficult to model. The time and effort could be reduced with tools automating the interaction between large BAS trend databases and building simulation software such as the AACS. Overall it is hypothesised that bottom-up calibration can create more accurate and reliable models than those using existing approaches.

Acknowledgements

The authors acknowledge financial support provided by the NSERC Smart Net-Zero Energy Buildings Strategic Research Network and the Faculty of Engineering and Computer Science (Concordia University).The first author gratefully acknowledges the ASHRAE Graduate Student Grant-In-Aid Award (2013-2014) and the NSERC Alexander Graham Bell Canada Graduate Scholarship.

References

ASHRAE, 2001. *ANSI/ASHRAE Standard 62-2001, Ventilation for Acceptable Indoor Air Quality,* ASHRAE, Atlanta, Georgia.

ASHRAE, 2002. *ASHRAE Guideline 14-2002, Measurement of Energy and Demand Savings,* ASHRAE, Atlanta, Georgia.

ASHRAE, 2009. *ASHRAE Handbook – Fundamentals,* ASHRAE, Atlanta, Georgia.

ASHRAE. 2010. *ANSI/ASHRAE/IES Standard 90.1-2010, Energy Standard for Buildings Except Low-Rise Residential Buildings*, ASHRAE, Atlanta, Georgia.

Carling, P, Isakson, P. Blomberg, P, & Eriksson, J, 2003. Experiences from evaluation of the HVAC performance in the Katsan building based on calibrated whole building simulation and extensive trending, viewed February, 2014. <http://www.commissioning-hvac.org/files/doc/A40-D-M6-SWE-%C3%85F_KTH-2.pdf>

Claridge, DE, Haberl, JS, Abushakra, B, & Sreshthaputra, A, 2004. Electric Diversity Profiles for Energy Simulation of Office Buildings, *ASHRAE Transactions,* vol. 110, no. 1, pp 365-77.

Davis, JA, & Nutter, DW, 2010. Occupancy diversity factors for common university building types. *Energy and Buildings* vol. 42, 1543-51.

Gestwick, MJ, & Love, JA, 2013. Trial application of ASHRAE 1051-RP: calibration method for building energy simulation, *Journal of Building Performance Simulation*, <http://dx.doi.org/10.1080/19401493.2013.838698>

Haves, P, Salsbury, T, Claridge, D, & Liu, M, 2001. Use of whole building simulation in on-line performance assessment: modelling and implementation issues, Proceedings of the 7th International IBPSA Building Simulation Conference, Rio de Janeiro, Brazil.

Heo, Y, Choudhary, R, & Augenbroe, GA, 2012. Calibration of building energy models for retrofit analysis under uncertainty, *Energy and Buildings*, vol. 47, pp. 550-60.

Kandil, AE & Love, JA, 2013. Signature analysis calibration of a school energy model using hourly data, *Journal of Building Performance Simulation*, <http://dx.doi.org/10.1080/19401493.2013.838608>

Lawrence Berkeley National Laboratory (LBNL) & James J. Hirsch & Associates (JJH), 1998. DOE-2.2, viewed January, 2013 <http://www.doe2.com/equest/>

Liu, M., Claridge, DE, Bensouda, N, Lee, SU, Wei, G, & Heinemeier, K, 2005. Manual of Procedures for Calibrating Simulations of Building Systems, Lawrence Berkeley Laboratory, Berkeley, California.

Liu, G, & Liu, M, 2011. Applications of a Simplified Model Calibration Procedure for Commonly used HVAC Systems, *ASHRAE Transactions*, vol. 117, no. 1, pp. 835-46.

NRC, 1997. *Model National Energy Code for Buildings*, National Research Council of Canada, Ottawa, Canada.

Mihai, A & Zmeureanu, R, 2013. Calibration of an energy model of a new research center building, Proceedings of the Thirteenth International IBPSA Building Simulation Conference, Chambery, France, pp. 1786-95.

Millette, J, Sansregret, S & Daoud, A 2011. SIMEB: Simplified interface to DOE2 and EnergyPlus – A user's perspective – Case study of an existing building, Proceedings of the Eleventh International IBPSA Building Simulation Conference, Sydney, Australia, pp. 2349-55.

Monfet, D, Zmeureanu, R, Charneux, R, & Lemire, N, 2009. Calibration of a Building Energy Model Using Measured Data, *ASHRAE Transaction*, vol. 115, no.1, pp. 348–59.

O'Neill, Z, Pang, X, Shashanka, M, Haves, P, & Bailey, T, 2013. Model-based real-time whole building energy performance monitoring and diagnostics, *Journal of Building Performance Simulation*, vol. 7, no. 2, pp. 83-99.

Raftery, P, Keane, M, & O'Donnell, J, 2011. Calibrating whole building energy models: An evidence-based methodology, *Energy and Buildings*, vol. 43, pp. 2356-64.

Reddy, TA, 2006. Literature Review on Calibration of Building Energy Simulation Programs: Uses, Problems, Procedures, Uncertainty, and Tools, *ASHRAE Transactions*, vol. 112, no. 1, pp. 226–40.

SIMEB, 2013. Simulation énergétique des bâtiments (SIMEB): Weather data, viewed October, 2013, <https://www.simeb.ca:8443/index_en.jsp>

Sun, J, & Reddy, TA, 2006. Calibration of Building Energy Simulation Programs Using the Analytic Optimization Approach (RP-1051), *HVAC&R Research*, vol. 12, no. 1, 177-96.

Torcellini, PA, Deru, M, Griffith, B Long, N, Pless, S Judkoff, R & Crawley, DB, 2006. Lessons Learned from Field Evaluation of Six High-Performance Buildings. National Renewable Energy Laboratory. Viewed December 2013, <http://www.nrel.gov/docs/fy06osti/37542.pdf>

Zibin, NF, Zmeureanu, RG, & Love, JA, 2013. Use of Building Automation System Trend Data for Inputs Generation in Bottom-Up Simulation Calibration, Proceedings of the Thirteenth Annual International Conference for Enhanced Building Operations, Montreal, Canada.